

# Multidimensional Nonlinear Registration: a Stochastic Formulation

Oleh J. Tretiak and Maria Gabrani

Imaging and Computer Vision Center, Drexel University, Philadelphia PA 19104, USA  
tretiak@coe.drexel.edu (215) 895 2214

## ABSTRACT

Many image processing applications require the comparison of images or multidimensional data sets. While rigid body transformations are in common use, applications in medicine and biology where images from different individuals are compared require nonlinear transformations. A number of investigators have explored nonlinear or 'rubber sheet' transformations, which have great expressive power. We develop a random field model for such transformations. Each transformation is a sample function from a random process. Maximum likelihood estimation of the transformation has a direct relation to radial interpolation theory. The stochastic process formulation provides a model that facilitates prediction of alignment accuracy. The theory is illustrated with application to three-dimensional alignment of brain images that arise in neuroscience research. The proposed transformations lead to algorithms that provide better accuracy.

## 1. INTRODUCTION

In an alignment task we are given two "images"  $f_1(\mathbf{x})$ ,  $f_2(\mathbf{x})$  defined over  $d$ -dimensional space. We are required to find a space transformation  $T(\mathbf{x})$  and to compute  $f_1'(x) = f_1(T(x))$  in which homologous points in  $f_1(x)$  and  $f_2(x)$  are aligned. In biomedical applications where volumetric studies ( $d=3$ ) from different individuals are aligned rigid-body transformations do not provide sufficient accuracy. Most of the work to date has been empirical: algorithms are proposed, and their efficacy is evaluated through empirical trials. In this research we propose a random process model for the deformations that are required to align biological objects. We feel that a suitable model can suggest better alignment algorithms, and predict the accuracy with which such alignment is possible. Our model has been motivated by a new class of nonlinear transformations, called elastic transformations [1]. The formulation is based on multidimensional spline theory developed by Duchon [2] and further developed by Meinguet [3]. Elastic transformations have a closed-form interpolation formula. The formulation follows the elastic deformation methodology introduced by Bajcsy et al. [4, 5], and further studied by Miller and co-workers [6], and Kass and his colleagues [7]. The above authors use

correlation of gray scale data to drive their registration. Our research is based on the use of geometric features extracted from the images, and is motivated by the interpolation theory introduced to this field by Bookstein [8]. The effectiveness of an interpolation technique is measured by the accuracy with which it predicts the values of the function at ordinates not used to compute the function. In the case of brain mapping, we measure how well inner structures of an atlas or reference image are mapped to the corresponding locations in a test image. To measure this accuracy we align a brain and its known second order polynomial transformation.

The paper is organized as follows. In the next section, we describe a model for the proposed transformations, and relate it to our elastic transformation algorithm. In the third section, we report results of alignment trials. In the last section, we discuss the relation between the results of these trials and the proposed model.

## 2. RANDOM TRANSFORMATIONS

We assume that the transformation between the two data sets has the following form:

$$T(\mathbf{x}) = \mathbf{x} + \mathbf{u}(\mathbf{x}) \quad (1)$$

where  $\mathbf{u}(\mathbf{x}) = \nabla \phi(\mathbf{x})$ . This definition is motivated by elasticity theory. The function  $\phi(\mathbf{x})$  is a sample function of a Gaussian random process with density function given by

$$f(\phi(\bullet)) = k \exp(-\int [w * (\phi - \mu)](\mathbf{x})^2 dx) \quad (2)$$

where  $w*$  represents the application of an operator described below (for example,  $w*$  may be equal to  $\Delta$ , the Laplacian operator), and  $\mu(\mathbf{x})$  is the mean of the random process. At present, we assume that  $\mu(\mathbf{x}) = 0$ . We assume that we are given two point sets  $S_1$  and  $S_2$  in the two images that are to be matched, so that  $T$  must satisfy

$$\mathbf{x} \in S_1 \Rightarrow T(\mathbf{x}) \in S_2. \quad (3)$$

For computational purposes, we approximate the above integral in the following way: we choose a set of  $N$  points  $\mathbf{A} = (\mathbf{a}_1, \dots, \mathbf{a}_N)$ ,  $\mathbf{a}_i \in S_1$  and look for points  $\mathbf{B} = (\mathbf{b}_1, \dots, \mathbf{b}_N)$ ,  $\mathbf{b}_i \in S_2$ . Function  $\phi$  must now satisfy the interpolation constraints

$$\mathbf{a}_i + (\nabla \phi)(\mathbf{a}_i) = \mathbf{b}_i, \quad i = 1, \dots, N. \quad (4)$$

and a function that satisfies (4) will be denoted as  $\phi(\mathbf{x}; \mathbf{A}, \mathbf{B})$ , and the likelihood of this function is  $f(\phi(\mathbf{x}; \mathbf{A}, \mathbf{B}))$ . We now find  $\phi$  and  $\mathbf{B}$  by the principle of maximum likelihood. For notational convenience, we



choose to work with  $Q = -\ln(f)$ , so that we need to solve the formal problem

$$\min_{\phi, \mathbf{B}} Q(\phi(\cdot; \mathbf{A}, \mathbf{B})) = \min_{\phi, \mathbf{B}} \int |w * \phi(\mathbf{x}; \mathbf{A}, \mathbf{B})|^2 d\mathbf{x}. \quad (5)$$

We seek a minimum over  $\phi$  in the space of temperate distributions.

To examine some of the implications of this formulation, we review some results presented in [1]. We write the integral in the Fourier domain,

$$Q(\phi(\cdot; \mathbf{A}, \mathbf{B})) = \int |\hat{w}(\xi) \hat{\phi}(\xi; \mathbf{A}, \mathbf{B})|^2 d\xi, \quad (6)$$

where  $\hat{w}$ ,  $\hat{\phi}$  are, respectively, the Fourier transforms of  $w$  and  $\phi$ . We assume that  $w$  is radially symmetric, so that  $\hat{w}(\xi) = g(\|\xi\|)$ , and that for  $\rho = \|\xi\| > 0$   $g(\rho) > 0$ ,

$$\lim_{\rho \rightarrow 0} g(\rho) = \rho^m, \quad \lim_{\rho \rightarrow \infty} g(\rho) = \rho^k. \quad (7)$$

The functions  $\phi(\cdot)$  for which the  $Q$  is zero (the kernel of  $Q$ ) is the linear space of polynomials of degree less than  $m$ . A minimum over  $\phi$  of (6) subject to the interpolation constraints (5) is achieved (in the space of temperate distributions) when  $k > d/2 + 1$  and when the point set  $\mathbf{A}$  contains a unisolvent subset for polynomials of degree  $m-1$ . The solution can be constructed as follows: let

$$p_j(\mathbf{x}), \quad j = 1, \dots, M, \quad M = C(d+m-1, d) \quad (8)$$

be a set of linearly independent polynomials of degree  $m-1$  in  $d$  variables. The function  $\mathbf{u}(\mathbf{x})$  is given by

$$\mathbf{u}(\mathbf{x}) = \sum_{i=1}^N \mathbf{H}(\mathbf{x} - \mathbf{a}_i) \cdot \boldsymbol{\gamma}_i + \sum_{j=1}^M d_j \nabla p_j(\mathbf{x}), \quad (9)$$

where  $\mathbf{H}(\cdot)$  is the tensor-valued function

$$H_{kl}(\mathbf{x}) = \frac{\partial^2 E(\mathbf{x})}{\partial x_k \partial x_l}, \quad (10)$$

$\boldsymbol{\gamma}_i$  are  $d$ -dimensional vectors, and  $E(\mathbf{x})$  satisfies the equation

$$\hat{E}(\xi) = \frac{1}{\hat{w}^2(\xi)}. \quad (11)$$

Coefficients  $\boldsymbol{\gamma}_i$ ,  $d_j$  are found from the interpolation constraints (4)

$$\mathbf{b}_k = \mathbf{a}_k + \sum_{i=1}^N \mathbf{H}(\mathbf{a}_k - \mathbf{a}_i) \cdot \boldsymbol{\gamma}_i + \sum_{j=1}^M d_j \nabla p_j(\mathbf{a}_k), \quad (12)$$

$k = 1, \dots, N$  and the orthogonality constraints

$$\sum_{i=1}^N \nabla p_j(\mathbf{a}_i) \cdot \boldsymbol{\gamma}_i = 0, \quad j = 1, \dots, M. \quad (13)$$

To summarize, the solution of the minimization of  $Q$  over  $\phi$  reduces to the solution of a set of linear equations. Define

$$Q(\mathbf{A}, \mathbf{B}) = \min_{\phi} Q(\phi(\cdot; \mathbf{A}, \mathbf{B})). \quad (14)$$

$Q(\mathbf{A}, \mathbf{B})$  is a quadratic function in the variables  $(\mathbf{b}_i)$ . The maximum likelihood solution to the estimation problem is found by locating

$$\min_{\mathbf{B} \in S_2} Q(\mathbf{A}, \mathbf{B}).$$

We now return to the probabilistic formulation of the problem. From a formal perspective, we would like to ask whether the problem is well-posed, i. e. under what conditions does the solution of (5) exist? The structure of the density function (2) implies that the random process  $(\phi - \mu)(\mathbf{x})$  is stationary, and its power spectrum is

$$S(\xi) = |\hat{w}(\xi)|^{-2}. \quad (15)$$

This spectrum is, typically, singular. For example, when  $d = 1$  and  $w = D$  (the differential operator) the process generating functions  $\phi$  is a random walk, and the variance of  $\phi$  is infinite. However, certain linear combinations of the random variables have finite variance. Specifically, if we define the random variable

$$\mathbf{z} = \sum_{k=1}^P c_k \mathbf{u}(\mathbf{a}_k), \quad (16)$$

and if the coefficients  $c_k$  satisfy the orthogonality constraints

$$\sum_{k=1}^P c_k p_j(\mathbf{a}_k) = 0, \quad j = 1, \dots, M, \quad (17)$$

then the variance of  $\mathbf{z}$  is finite, and is furthermore given by the equation

$$V(\mathbf{z}) = \sum_{k=1}^P \sum_{l=1}^P c_k c_l E(\mathbf{a}_k - \mathbf{a}_l), \quad \hat{E} = S. \quad (17)$$

We see that this framework is well adapted for interpolation problems.

## EXPERIMENTS

We examine the performance of the proposed transformation method in the alignment of rat brains. Our research deals with the development of tools for neuroscience studies. Inbred laboratory rats are a standard model for neurochemistry research, since the low genetic variability allow easy experimental designs in which treatment effects, such as the response of the brain to neuroactive drugs, can be separated from intra-individual variability. The large amount of published data for this model also make it attractive for further experimental studies. Autoradiographic measurement of metabolic activity, neurotransmitter distributions, and protein synthesis with in-situ hybridization of mRNA produce voluminous data in the form of sectional images, and it is desirable to transform these images into a standard coordinate system for inter-animal comparisons.

We have developed a technique that aligns rat brains by using rigid-body [9] and affine [10] transformations based on distance between brain surfaces. The surface of the brain is a reliable feature which can be extracted from the images produced by most labeling methods. The accuracy of the technique is tested by comparing how well internal structures are aligned. We found [10] that the rigid-body and affine transformations produced a median error of about 168  $\mu\text{m}$  in the alignment of brain surfaces, and an error of



about voxels 88  $\mu\text{m}$  for various internal structures. In these experiments, the locations of these internal structures were not known to the alignment algorithms. ALIGN, a MATLAB implementation of this algorithms, is available through the web (<http://coe.drexel.edu/ICVC>). Though these results are encouraging, they were obtained with very precise techniques for preparing the rat brains. In usual practice more variability is encountered.

To test the effectiveness of surface-guided alignment we used a brain dataset from the above study, and distorted it with a second-order polynomial transformation. The ALIGN program was used to register the two brains with rigid body and affine transformations. The accuracy of these methods were compared with the results of an elastic transformation. In all cases, the surfaces of the brains provided the data for alignment. Note that the rigid-body and affine transformations are not interpolatory, they can not achieve perfect alignment of the brain surface. We measured the accuracy with which all algorithms registered the brain surface, an internal structure, as well as the accuracy with which the control points ( $\mathbf{a}_i$  in the above discussion) were aligned with their known images. The distance between sections in the data set was 100  $\mu\text{m}$ , and the thickness of each section is approximately 40  $\mu\text{m}$ .

The outer surface of the rat brain is shown in Fig. 1 (a), the transformed brain surface is in Fig. 1 (b), and the two datasets are superimposed in Figure 1(c). The outcomes of the rigid body, the affine and the elastic transformations are given in Figure 1 (d), (e) and (f), respectively. In all cases  $N = 40$  control points were used. It is evident that the best alignment is produced by the elastic transformation.

Numerical evidence of the performance is given in Table 1, where we provide the median Euclidean distance error in pixels between the target image and the outcomes of the transformations. In addition to the distance for the outer surface, we compute the median distances for the following internal structures: the third and fourth ventricles (V34), middle cerebellar peduncle (MCP), lateral ventricle (LV), midline of the cerebrum (MC), seventh nerve (N7), trigeminal nerve (TG5), corpus callosum (CC), cerebellar tracks (CT), and superior colliculus (SC).

**Table 1.** Median distance error (pixels) between the target image and the outcomes of alignment algorithms. One pixel = 42  $\mu\text{m}$ .

	Original	RB	AFF	ET
Outer Surface	30.23	19.5	3.4	2.2
V34	30.63	14.6	1.1	1
MCP	24.12	17.4	2.8	2.4
LV	26.9	14.0	1.6	1
MC	28.55	15.3	1.8	1.4
N7	29.18	16.8	4.2	2.4
TG5	29.92	20.0	4.9	2.4
CC	28.98	16.6	1.5	1
CT	32.52	10.7	3.8	1
SC	34.35	18.9	1.7	1

Knowing the exact correspondence of the control points we are able to examine the accuracy with which the algorithm locates them. Table 2 gives the energy between the initial point configuration and the final control points of the alignment algorithms. The known correspondence points give an energy  $Q$  of 0.0309. The estimation algorithm gives control points with energy 0.0357, which is very close to the minimum. The rigid-body and affine transformations produce control points with higher energy. However, the main criterion of performance is not the energy but the outcome registration quality of the algorithms. In Table 3 we give the median and mean distance error of the outcome of the elastic transformations considering the known correspondence and that found by the estimation algorithm. Notice that the difference is very small. The median errors are almost all the same, and the mean errors differ mainly in the second decimal point. The above results establish the use of the proposed surface based interpolation technique.

**Table 2.** Energy defined from the distance between the points in the original image and the final control points of the alignment

Control Points	Energy
Known Correspondence	0.0309
Elastic Estimation	0.0357
Affine	0.0829
Rigid Body	1.0454

**Table 3.** Distance error (pixels) between the target image and the outcomes of elastic transformations with known correspondence and estimating control points locations.

Error	Known		Estimated	
	Median	Mean	Median	Mean
Outer Surface	2.2	1.6	2.2	1.6
V34	1	0.8	1	0.9
MCP	2.4	2.5	2.4	2.6
LV	1	0.8	1	0.8
MC	1.4	1.7	1.4	1.8
N7	2.2	2.6	2.4	2.7
TG5	2.2	2.2	2.4	2.3

## 4. DISCUSSION

We have developed a multidimensional alignment algorithm that is based on multidimensional interpolation theory [2, 3], and that can furthermore perform an effective transformation when only the surfaces of the objects are known (no known point correspondences). In this paper we show that the algorithm has a natural relationship to a random process formulation of multidimensional alignment. In the future we propose to further explore the implications of the random process model. For example, both the alignment algorithm and the random process make essential use of the interpolating function  $E(\bullet)$  defined in (11) which depends on the smoothness operator  $w$ . In the interpolation theory this function is ad-hoc, while the random process theory indicates that this is the Fourier transform of the power spectrum. This suggests that the



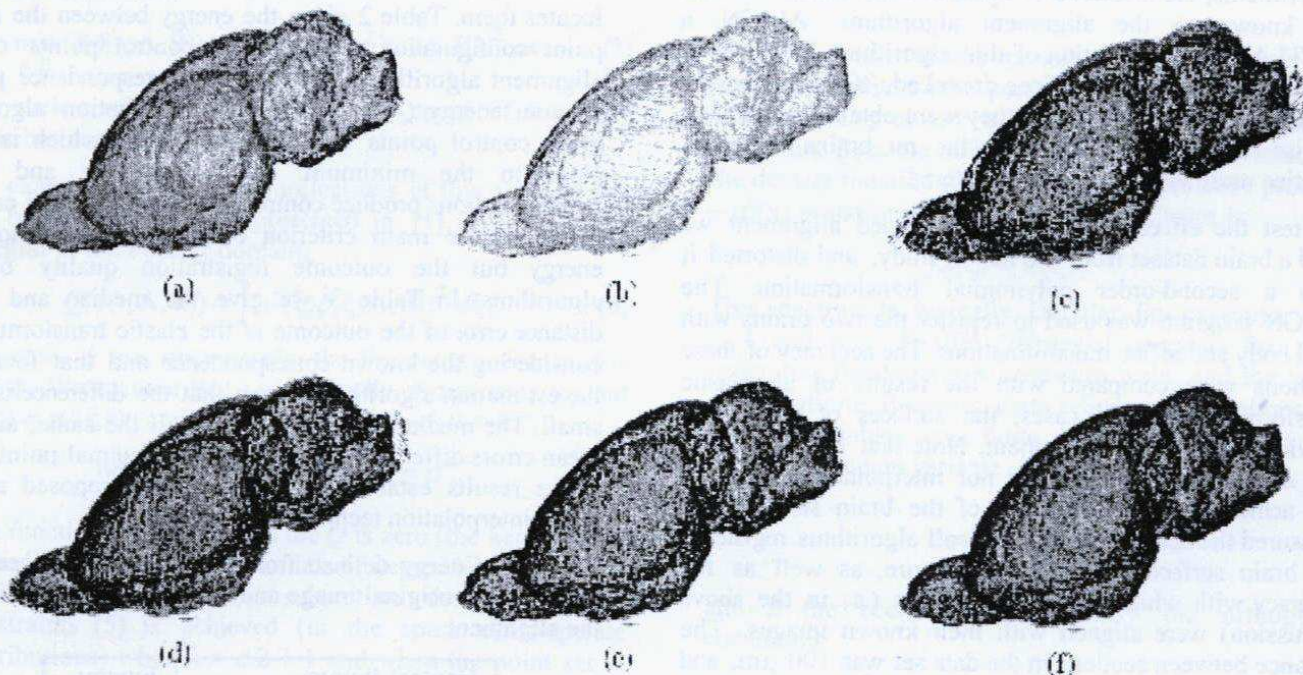


**Figure 1.** (a) Surface of a rat brain, (b) the same dataset, transformed with a quadratic polynomial, (c) for comparison, the two brains superimposed, (d) rigid body alignment, (e) affine, and (f) elastic transformation.

appropriate  $w$  can be found by performing experiments which measure the fluctuations in the interpolating transformation (found by some other method), and by deducing the form of  $E$  from these measurements. Another feature suggested by the random process model is inclusion of the random process mean  $\mu(\bullet)$  in the likelihood function (2). The inclusion of this function may lead to improvements in the alignment algorithm. Finally, the random process model can lead to analytical predictions about the magnitude of alignment errors. This may be of considerable value in making optimal choices of the control points  $\mathbf{a}_i$ . We expect that the accuracy of alignment will depend on both  $S(\bullet)$ , the random process spectrum, and on  $\mathbf{A}$ , the control point set. Choosing a larger control point set will improve accuracy of prediction of internal structure location until the limit of natural variability is reached. The proposed theory may allow us to identify this point of diminishing returns.

**Acknowledgments.** This work is supported by NIH Grant P41-RR01638. We would like to express our thanks to Dr. Jonathan Nissanov, Dr. Cengizhan Ozturk, and Ms. Louise Bertrand for their graceful assistance.

## REFERENCES

- [1] Gabrani, M.; and Tretiak, O. J., "Surface Based Matching using Elastic Transformations," *Pattern Recognition*, in press.
- [2] Duchon, J., "Interpolation des fonctions de deux variables suivant le principe de la flexion des plaques minces," *RAIRO Analyse Numérique*, vol. 10, pp. 5-12, 1976.

- [3] Meinguet, J., "Multivariate Interpolation at Arbitrary Points Made Simple," *Journal of Applied Mathematics (ZAMP)*, vol. 30, 1979.

- [4] Broit, C., "Optimal registration of deformed images," Doctoral dissertation, Univ. Pennsylvania, 1981.

- [5] Bajcsy, R.; and Kovacic, S. "Multiresolution Elastic Matching." *Computer Vision, Graphics, and Image Processing*, vol. 46, pp. 1-21, 1989.

- [6] Miller, M.; Christensen, G.; Amit, Y.; and Grenander, U., "Mathematical textbook of deformable neuroanatomies," *Proc. Natl. Acad. Sci. USA*, vol. 90, pp. 11944-11948, December 1993.

- [7] Kass, M.; Witkin, A.; and Terzopoulos, D., "Snakes: Active contour models," *Int. J. Comput. Vision*, vol. 1, pp. 321-331, 1987.

- [8] Bookstein, F.L., "Principal Warps: Thin-Plate Splines and the Decomposition of Deformations," *IEEE trans. on PAMI*, vol. 11, no. 6, June 1989.

- [9] Kozinska, D.; Tretiak, O. J.; Nissanov, J.; and Ozturk, C., "Multidimensional Alignment Using the Euclidean Distance Transform," *Graphical Models and Image Processing*, vol. 59, November, pp. 373-387, 1997.

- [10] Ozturk, C., "Rat Brain Variability, Utility of its Surface for Guiding Alignment and Development of A Structured Light Based Brain Surface Scanner," Doctoral dissertation, Drexel Univ., 1997.